Numerical **Weather Prediction**

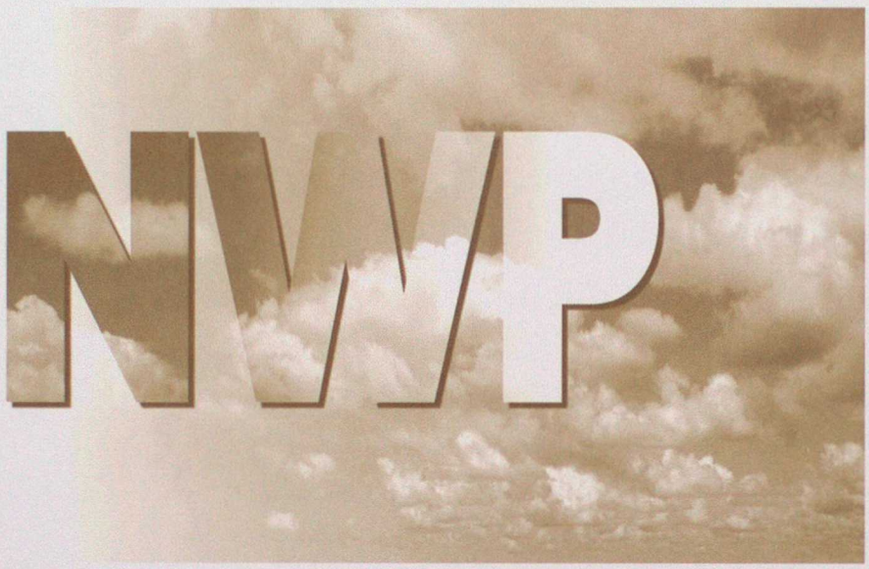

Forecasting Research
Scientific Paper No. 55

The Statistical Structure of Forecast Errors and its Representation in The Met. Office Global 3-Dimensional Variational Data Assimilation Scheme.

by

N.B. Ingleby

November 1999

The Met.Office

Excelling *in weather services*

Forecasting Research
Scientific Paper No. 55

The Statistical Structure of Forecast Errors and its Representation in The Met. Office Global 3-Dimensional Variational Data Assimilation Scheme.

by

N.B. Ingleby

November 1999

Meteorological Office
NWP Division
Room 344
London Road
Bracknell
Berkshire
RG12 2SZ
United Kingdom

Please notify us if you change your address or no longer wish to receive these publications.

Tel: 44 (0)1344 856245 Fax: 44 (0)1344 854026 e-mail: jsarmstrong@meto.gov.uk

Q. J. R. Meteorol. Soc. (9999), **999**, pp. 1–999

The Statistical Structure of Forecast Errors and its Representation in The Met. Office Global 3-Dimensional Variational Data Assimilation Scheme.

By N. Bruce. Ingleby*

The Meteorological Office, UK

(November 4, 1999)

SUMMARY

Previous studies and different methods of estimating short-range forecast errors are summarised. Statistics based on differences of 1- and 2-day forecasts valid at the same time are presented and an attempt is made to explain many of the features by reference to dynamical concepts.

Vertical correlation length scale tends to increase with horizontal correlation scale but to be very short in the tropics; horizontal scale is longest in the tropics and in the stratosphere. The variations in vertical correlation are much more pronounced for largely balanced variables such as rotational wind and temperature than they are for divergent wind or humidity. The extratropics are dominated by an equivalent barotropic mode with the level of the maximum wind amplitude (and the zero crossing of the temperature correlation) being determined by the tropopause. One surprising feature is that surface pressure and low level temperature are positively correlated over the Antarctic plateau.

The covariance model used in the Met. Office Global 3-Dimensional Variational (3D-Var) Data Assimilation System (Lorenc *et al.*, 2000) represents the variation of vertical covariances with latitude reasonably well, but the longer horizontal scales in the stratosphere are not currently reproduced. The implied covariances used operationally have been modified so that the correlation length scales, both horizontal and vertical, are somewhat shorter than those direct from the forecast differences. Recent changes to the representation are briefly described, with an indication of their impact on the forecasts. The impacts are significant relative to other changes tested, and the covariance model has played a major role in the successful implementation and subsequent improvement of our 3D-Var system.

KEYWORDS: forecast errors, error covariances, variational data assimilation

1. INTRODUCTION

(*a*) *Overview*

Atmospheric data assimilation systems combine information from observations and a short-range (typically 6 hour) forecast referred to as the 'background'. Estimates are needed of the observation and background error covariances. The background error covariance estimates are important, particularly in data sparse regions, as they determine the spreading of information between the observation locations and also multivariate balance relationships. The covariances are often decomposed into correlations, assumed to be constant globally or over large regions, and standard deviations which are allowed more geographical variation. Daley (1991) provides an overview of this field.

Estimating the forecast error covariances is not straightforward as we never have the truth available, only different approximations to it. The remainder of section 1 summarises the different ways of estimating background error covariances, the results of previous studies and physical relationships between horizontal and vertical length scales. Section 2 shows the covariances estimated directly from forecast differences and concentrates particularly on the vertical structure and its variation with latitude. Section 3 describes the representation the background errors within our 3D-Var system, recent modifications and selected results of analysis/forecast experiments.

(*b*) *Forecast errors - determining factors and evolution*

* Corresponding author: Meteorological Office, London Road, Bracknell, Berkshire, RG12 2SZ, UK.

Forecast errors depend on the observations available, the data assimilation system and the forecast model; they also vary with the synoptic and seasonal situation. In 'sensitive' areas the forecast errors may grow rapidly whereas in other areas the errors may grow slowly or even decay initially. The analysis/forecast systems of operational forecasting centres are sufficiently good (or sufficiently similar) that their forecast error statistics have much in common.

Boer (1994) differentiates three regimes of forecast skill. The large-scale regime (global wavenumber $n < 10$) is dominated by stationary (largely zonal) structures that are relatively uncontaminated by error in forecasts out to 10 days. The synoptic scales ($10 < n < 80$) exhibit classical predictability behaviour in which error, initially concentrated at smaller scales, penetrates up the spectrum and saturates at values roughly twice the observed variance. Thus there is some similarity between the covariances of short-range forecast error and of observed fields, but the latter have rather longer scales. Somewhat surprisingly high wavenumbers ($n > 100$) exhibit some forecast skill out to 10 days - due to local topographic forcing.

In practice we are largely concerned with errors in the synoptic scales, so that forecast error length scales tend to increase as the length of the forecast increases. Initially this will be most noticeable in data dense areas which have shorter analysis error length scales than data sparse areas. Thus using differences between longer period forecasts to estimate background errors we may overestimate the length scales, particularly for data dense areas.

(*c*) *Previous studies*

Until recently the main way of estimating background error was by comparison with observations. The observation errors were assumed to be uncorrelated so that any spatial correlation was due to the forecast error. In this way Hollingsworth and Lönnberg (1986) and Lönnberg and Hollingsworth (1986) investigated the structure of wind and height errors using the North American radiosonde network. They found that the background errors were comparable in magnitude to the observation errors. Forecast errors were dominated by synoptic scale rotational wind and height perturbations in approximate geostrophic balance. There were some problems with the separability assumption (treating correlations as the product of horizontal and vertical correlation functions); in particular horizontal length scales were significantly longer in the stratosphere. Work elsewhere largely confirmed these features. For example Bartello and Mitchell (1992) concentrated on the increase of horizontal scale with height.

Ghil *et al.* (1979) and Mitchell *et al.* (1990), comparing forecasts with satellite temperatures and radiosonde heights respectively, found some evidence of shorter horizontal length scales at higher latitudes. Dee and Gaspari (1996), using forecast differences, found longer horizontal scales for height in the tropics. The variation of horizontal scale with latitude was examined using stochastic-dynamic models by Balgovind *et al.* (1983) and Jiang and Ghil (1993). Both papers conclude that horizontal scales vary in a similar way to the Rossby radius of deformation - but they take the scale height to be independent of latitude. In data dense areas error variances will be smaller, length scales generally shorter and the covariances will be more isotropic and less dependent on the dynamics (Bouttier, 1994).

The Met. Office's previous data assimilation system, the Analysis Correction (AC) scheme (Lorenc *et al.*, 1991), had longer horizontal scales in the tropics and southern hemisphere. Based on unpublished studies both the AC and the ECMWF Optimal Interpolation analysis systems used narrower vertical correlations in the tropics. Ingleby and Bromley (1990) compared wind error covariances for two different areas and two different

horizontal resolutions of the Met. Office forecast system and found that the upstream data density appeared to make more difference than the model horizontal resolution.

Parrish and Derber (1992) introduced the use of forecast differences as a proxy for forecast errors (used here in sections 2 and 3). Rabier *et al.* (1998) noted sharper vertical correlations at smaller horizontal scales using this so-called "NMC method".

The three main ways of estimating forecast errors each have their own strengths and weaknesses. Comparison with observations is the only independent calibration available, but the observation errors have to be taken into account and, more importantly, there are severe limitations on the information available for data sparse areas. Stochastic-dynamic or Kalman Filter methods are powerful tools, but necessarily include an approximate model error term and may not treat non-linear error saturation correctly. The use of forecast differences is somewhat heuristic. In practice it provides reasonable estimates of forecast error in a form suitable for use in variational analysis systems. However the variances need rescaling (by coincidence the factor is often near one *), and in data sparse areas the variances may be underestimated. In data dense areas the length scales will tend to be overestimated as mentioned above. Also the effects of any model biases will be underestimated.

(*d*) *Horizontal and vertical length scales*

In the studies mentioned above and in our forecast difference statistics (section 2) it was found that vertical correlations of rotational wind and temperature (largely 'balanced' variables) vary strongly with both horizontal scale and latitude, but most other variables show much less variation of the vertical correlation. The physical explanation for this outlined below is largely taken from Lindzen and Fox-Rabinovitz (1989). Note that for forecast errors it will be modified by data density considerations as already discussed.

For quasi-geostrophic ('balanced') flow on a beta-plane the horizontal scale ΔL (Rossby radius of deformation) is related to the vertical scale Δz by

$$\Delta L = (N/f_0)\Delta z \tag{1}$$

where f_0 is the characteristic Coriolis parameter. This suggests that Δz will increase both as ΔL increases and as higher latitudes are approached, and is consistent with larger ΔL in the more stable stratosphere. Near the equator

$$(\Delta L)^2 = (N/2\Omega)\Delta z a \tag{2}$$

where Ω is the earth's rotation rate and a its radius. Consistent with these equations we observe both small Δz and large ΔL in the tropics. For gravity waves there are less clear theoretical relations between vertical scale and either horizontal scale or latitude, but divergent wind and ageostrophic pressure may be weakly coupled with the balanced flow and show some of its characteristics.

The analysis above is relevant for free dynamics and may be modified by any forcing applied. It also neglects β and mean flow effects, these are summarised in equation 1 of Charney (1969). In particular the transmission of large amounts of energy from the troposphere into the upper atmosphere is prevented through most of the year (except near the equinoxes) by easterly or large westerly winds above the tropopause, and the transmissivity of the stratosphere increases with wavelength (Charney and Drazin, 1961). This appears to be the main reason for longer horizontal length scales in the stratosphere

* We currently take it to be 1.0, Rabier *et al.* scale their standard deviations by 0.9.

and in particular the continued increase in length scale above 100 hPa (the larger value of N in the stratosphere will also play a role but it is almost constant above 100 hPa, see table 1 and Fig. 3 in next section). In an analagous way disturbances propagating from mid-latitudes into the tropics will tend to be confined to the high troposphere and lower stratosphere where the zonal winds are weak easterly or westerly (see Charney (1969) and Tomas and Webster (1994)).

2. Forecast difference covariances

(*a*) *Horizontal covariances*

The statistics shown here (apart from Fig. 3) are all taken from differences of T+24 and T+48 operational forecasts (valid at the same time) for 29 days each in July 1998 and January 1999, those showing variation with latitude are for January 1999, except Fig. 1. As already stated such forecast differences are an imperfect proxy for forecast errors, brief validation of some aspects against observation minus background statistics is mentioned below, but a fuller comparision is outside the scope of the current work.

Until January 1998 the forecast model (described by Milton and Wilson (1996)) was run at 19-levels on a 1.25° longitude by 0.833° latitude grid; it was then upgraded to 30-levels, 0.833° longitude by 0.556° latitude grid spacing. During the development of our 3D-Var system forecast difference covariances have been calculated for several different periods and for both resolutions. The statistics have been fairly consistent, some exceptions are noted below. The temperature and humidity fields have been interpolated onto a staggered Charney-Phillips grid in the vertical and we convert the T+24 pressure-based vertical grid into a height coordinate grid as explained in Lorenc *et al.* (2000) section 2f. For storage reasons all fields have been interpolated onto the previous 1.25° by 0.833° horizontal grid — for the spectral statistics they were transformed to spectral T143 resolution. The control variables used in our 3D-Var system are: streamfunction, ψ; velocity potential, χ; unbalanced pressure, denoted Ap (essentially ageostrophic pressure, see Lorenc *et al.* (2000) section 3b for details); and relative humidity, RH. Other variables used below are total pressure, p; temperature, T; and wind components, (u, v). All the figures are presented on model levels.

Let the spectrum of the streamfunction be given by $D_n(\psi)$, where n is the global wavenumber, $D_n(\psi)$ is essentially the variance at that wavenumber (normalised by the total variance in the case of a correlation spectrum). The Rotational Kinetic Energy at that wavenumber is given by $RKE_n = 0.5D_n(\psi)n(n+1)/a^2$, and the vorticity spectrum is $D_n(\zeta) = D_n(\psi)n^2(n+1)^2/a^4$, (Boer, 1983). The differential length scale for ψ is given by $(2\sum D_n(\psi)/\sum(D_n(\psi)n(n+1)))^{0.5}$ and so is directly proportional to the square root of the ratio between streamfunction variance and RKE. Similar relationships apply to velocity potential, Divergent Kinetic Energy (DKE) and divergence. The forecast differences have significant variance of ψ and χ at large wavelengths (small n), but the associated wind is rather small. For this reason the RKE and DKE length scales below are felt to be more meaningful than those for ψ and χ.

The differential length scales in table 1 all show the well known increase with height in the stratosphere (see sections 1c and 1d). There is also a secondary maximum at approximately 800 hPa, particularly for velocity potential, the reasons for this are unclear. One might expect slightly shorter scales very close to the surface, this is seen to a limited extent. In moving from 19- to 30-levels horizontal scales of most variables reduced by about 20% in mid-troposphere and by 35% or more at 100 hPa — the scales in the stratosphere were presumably constrained by the vertical resolution.

TABLE 1. DIFFERENTIAL LENGTH SCALES (KM) FOR FORECAST DIFFERENCES, SELECTED MODEL LEVELS.

level	P	ψ	RKE	χ	DKE	Ap	RH	p	T
28	30	1353	366	1879	418	977		893	756
25	102	1057	277	1343	282	611	234	683	409
19	251	670	273	983	222	490	207	541	297
11	519	599	229	827	179	495	174	500	282
4	867	628	217	1045	195	536	171	499	251
2	961	581	199	724	181	433	164	466	211

Data for July 1998 and January 1999 combined.
The second column gives the average pressures in hPa for the levels. Due to the vertical grid staggering T and RH are at slightly lower average pressures than those indicated.

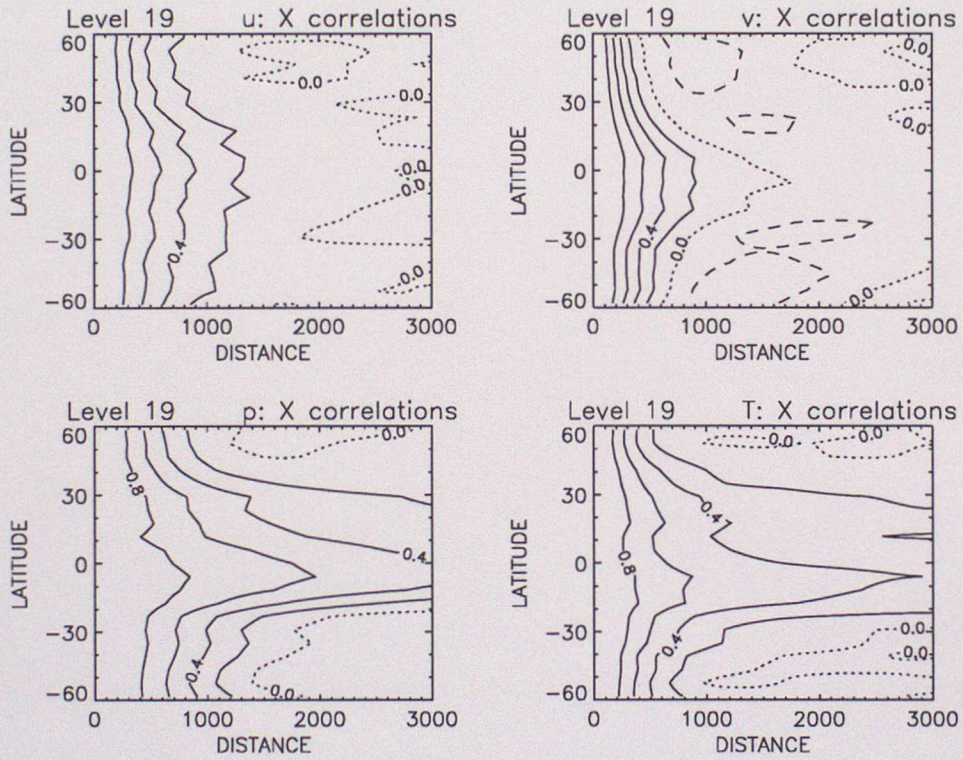

Figure 1. E-W horizontal correlation against distance (km, along the parallel of latitude), for level 19, approx. 250 hPa, July 1998. a) u wind, b) v wind, c) pressure and d) temperature.
Contour interval 0.2, with positive contours solid, zero contour dotted and negative contours dashed.

East-West correlations for July and latitudes between 60° N and 60° S are shown in Fig. 1. (These grid-point statistics are not used in our 3D-Var system where the spectral representation implies that the horizontal correlations are homogeneous and isotropic for each vertical mode.) The most notable feature is that the correlations are broadest in the tropics particularly for pressure and temperature. The North-South correlations (not shown) are also longer in the tropics, but not by as much. The temperature and pressure differences in the tropics appear to have large scale biases because the correlations remain

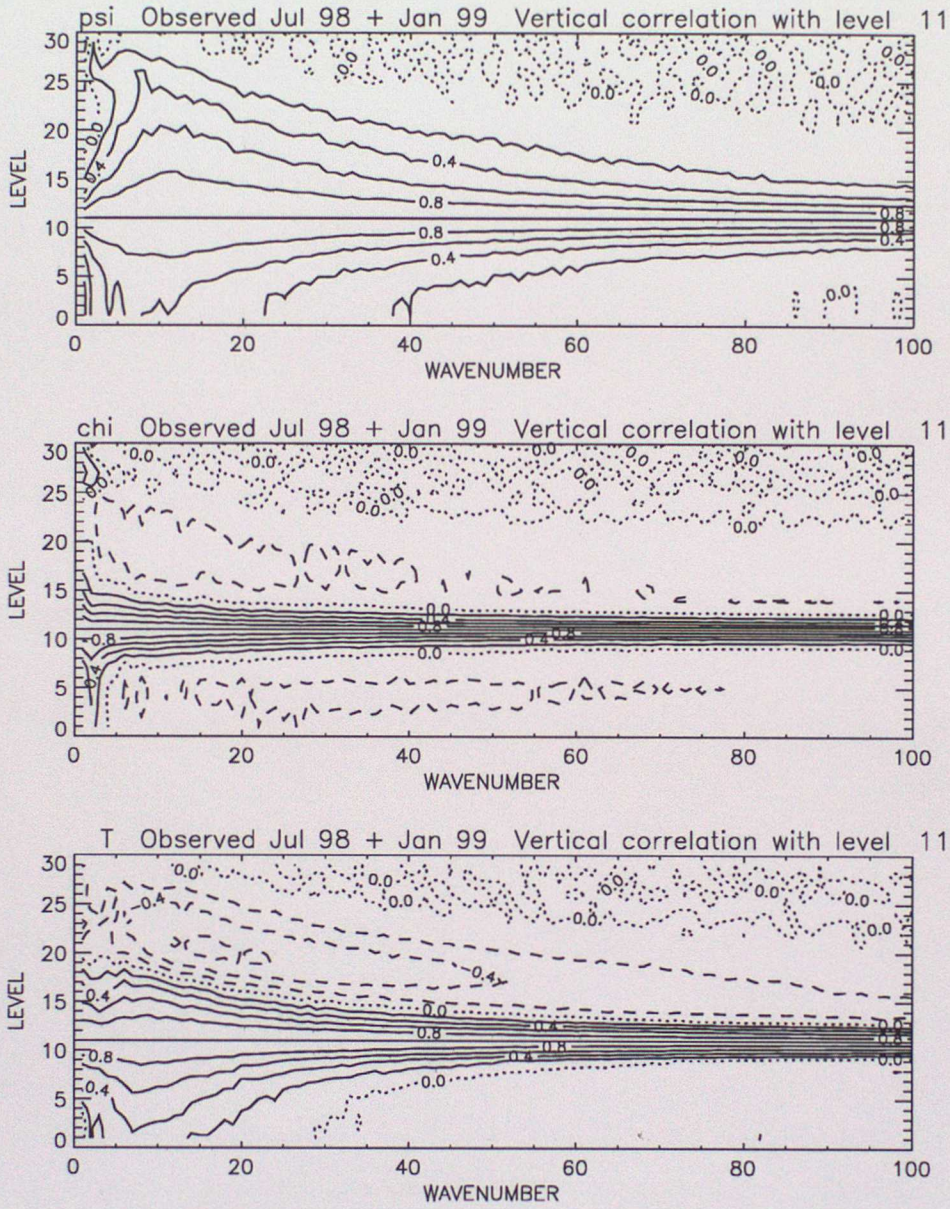

Figure 2. Vertical correlation as a function of horizontal wavenumber, July 1998 and January 1999 combined. a) rotational wind, b) divergent wind, c) temperature

positive and fairly flat out to 3000 km. For most of the variables there is some change of correlation shape with latitude — the curves are not described adequately by a single length scale.

In July the correlations are longer scale in the Southern extratropics than in the Northern extratopics. In January (not shown) the extratropical correlations are similar in both hemispheres and intermediate between the Northern and Southern July correlations. This corresponds to what one might expect: on average longer scales in the more data-

sparse and oceanic Southern mid-latitudes and in winter when the large scale forcing is more dominant. In the tropics the very longest scales tend to be just within the winter hemisphere. Streamfunction (not shown) has similar correlations to p, but not as broad in the tropics. Velocity potential (not shown) has rather different characteristics to the other variables examined, with largest scales at the poles. There is some indication that within the extratropics, correlation scales decrease slightly at higher latitudes, consistent with Eq. (1). However any latitudinal and seasonal variations in the extratropics are much less than the differences from the tropics.

Figure 2 shows the vertical correlations with level 11 (approximately 500 hPa) as a function of n, the global wavenumber. Note that Fig. 2a is valid for streamfunction, RKE and vorticity — for each n they have the same correlation matrix, but different variances (similarly for velocity potential, DKE and divergence in Fig. 2b). Apart from global scales ($n < 10$, where the term involving β and mean flow becomes important), streamfunction and temperature vertical scales decrease with horizontal scale, in qualitative agreement with Eq. (1). Streamfunction vertical correlations are very broad at large scales (except $n < 5$) and are essentially non-negative at all scales. Pressure vertical correlations (not shown) are qualitatively similar, but show signs of broadening again, particularly into the stratosphere, for $n > 80$. Temperature vertical correlations are narrower and show a significant negative lobe above for $10 < n < 50$.

Apart from $n < 8$ velocity potential vertical correlations are very narrow, and narrow more with increasing n, with slight negative lobes. Relative humidity vertical correlations (not shown) also show gradual narrowing with increasing n, at least for $n > 15$.

(*b*) *Vertical covariances*

Daley (1991, section 4.7) notes that "the vertical aspects of objective analysis have never been very satisfactory". In our 3D-Var system the vertical aspects are rather more sophisticated than the previous AC scheme, but are lacking a theoretical basis. The presentation here is a first step towards that.

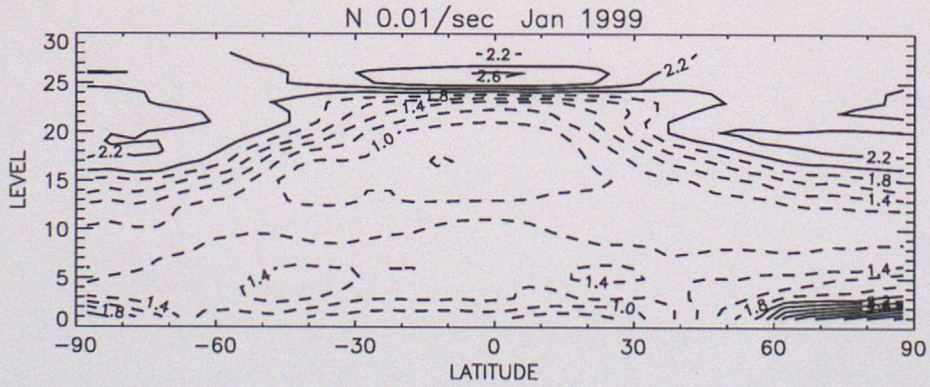

Figure 3. Brunt-Väisälä frequency N, units of 0.01 s^{-1}. T+24 forecasts, January 1999.

Figure 3 sets the scene showing the Brunt-Väisälä frequency N from the T+24 forecast zonal mean temperatures. N is slightly greater than 0.01 s^{-1} throughout much of the troposphere with minima (below 0.01 s^{-1}) in the tropics between approximately 450

and 200 hPa and also near the surface. At high latitudes the stability is higher near the surface, particularly near the winter pole with its low level inversion. Values in the stratosphere are typically about 0.02 s^{-1} with the tropopause height clearly varying with latitude. Apart from changes of tropopause height and polar inversions there is little seasonal variation of N, but stability tends to be slightly lower over continents in summer.

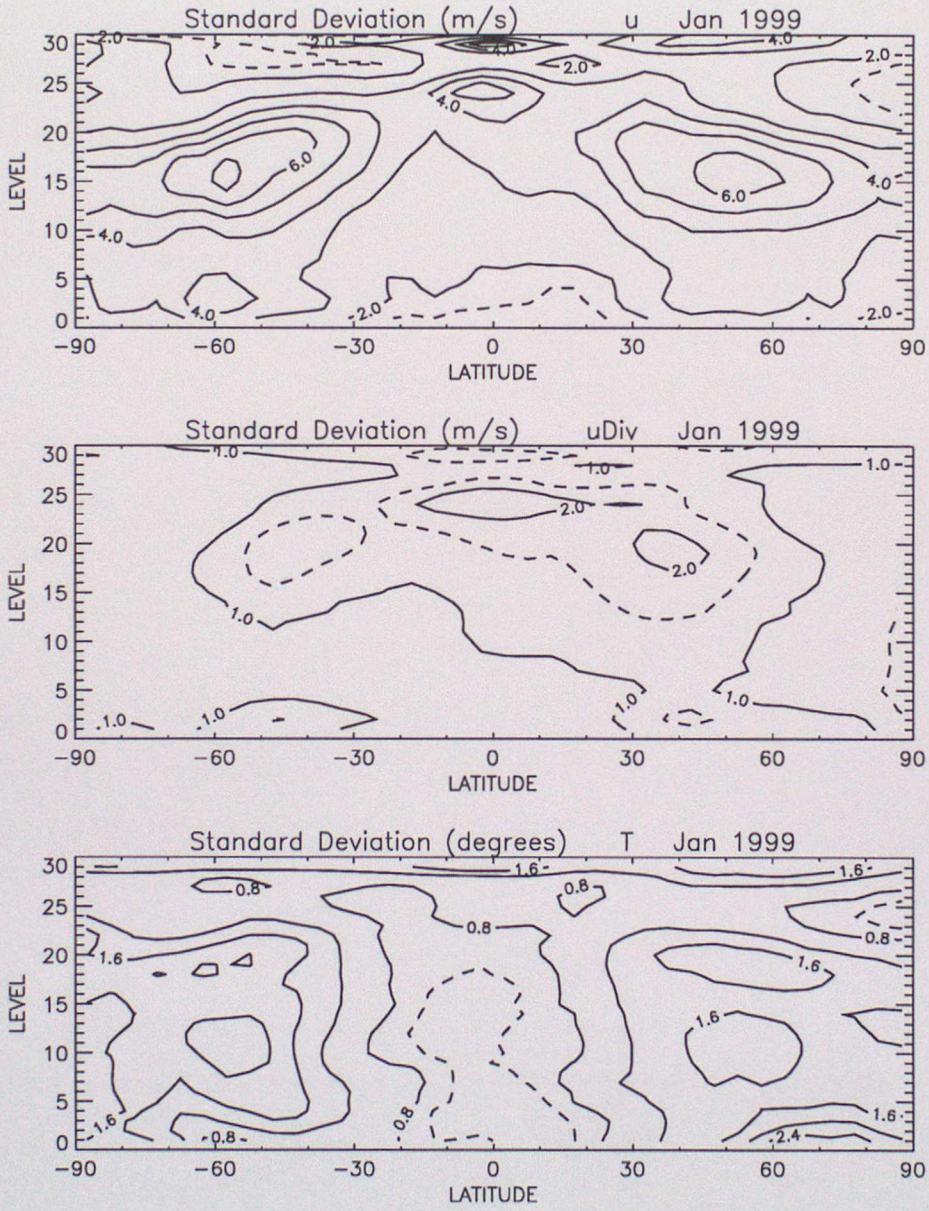

Figure 4. Standard deviations of forecast differences for January 1999. a) u, contours every 1 ms^{-1} with extra dashed contours at 0.5 and 1.5 ms^{-1}, b) as a but for u_{div}, c) temperature, contours every 0.4°with extra dashed contour at 0.6

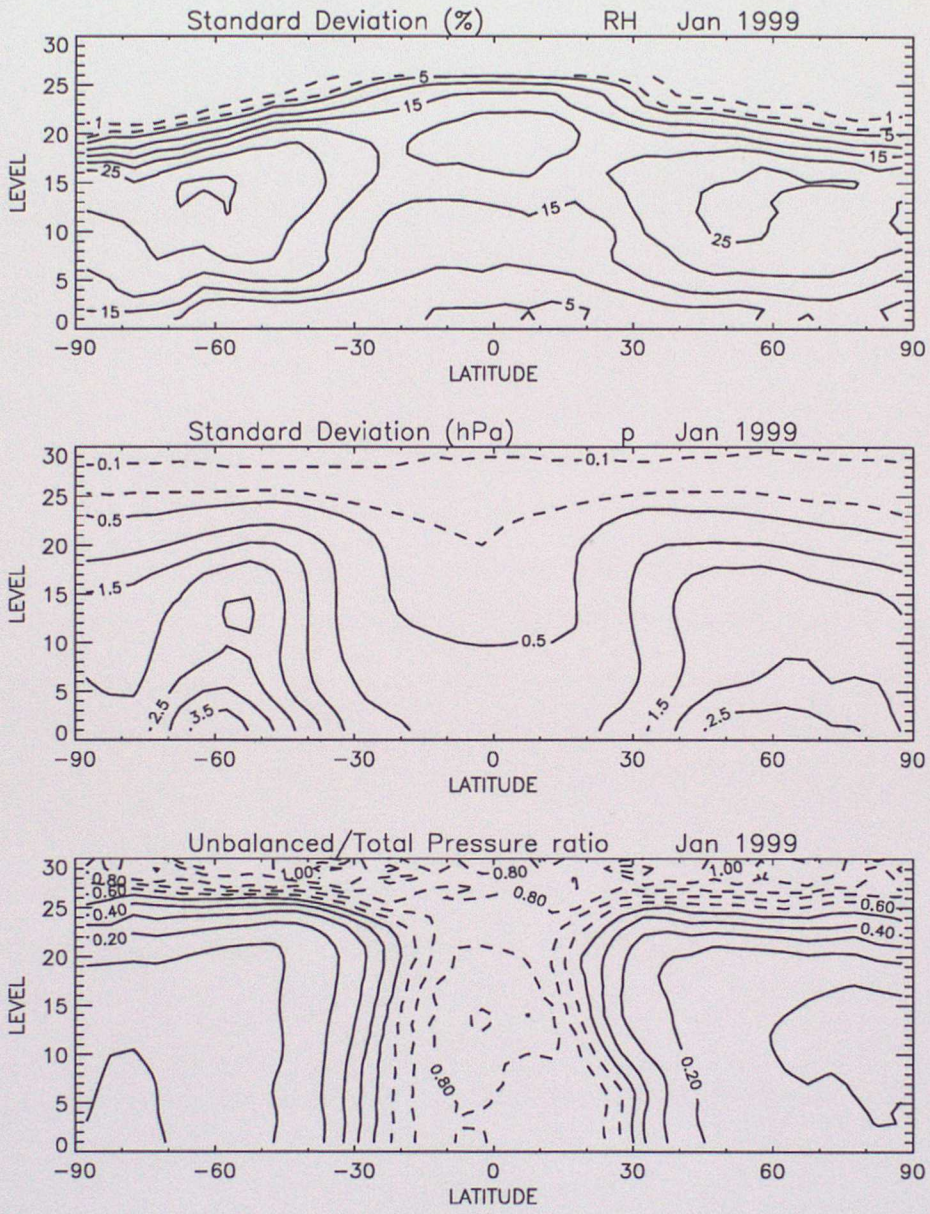

Figure 4. continued d) relative humidity in %, contours every 5% extra dashed contours at 1 and 3%, e) pressure in hPa, contours every 0.5 hPa extra dashed contours at 0.1 and 0.3 hPa, f) ratio of variances: unbalanced pressure/total pressure.

The standard deviation (SD) of the westerly wind component u (Fig. 4a) has maxima in mid-latitudes close to the tropopause and sloping upward towards the sub-tropics. There are generally smaller SDs in the tropics and in the stratosphere, although at high levels there are two localised maxima centred on the equator. The v component (not shown) has very similar vertical covariances, with slightly smaller magnitude in the tropics but slightly larger mid-latitude maxima. The SD of u_{div} (the u component

of the divergent wind, Fig. 4b) is generally much smaller, illustrating that the wind is largely rotational. Largest values are at high levels particularly in the tropics. The divergent wind shows more variability with sample than other variables examined and the tropical maximum at about 125 hPa became more pronounced after the introduction of a parametrization of convective momentum transport.

Temperature (Fig. 4c) has broad maximum SDs in the mid-latitude troposphere, extending into the lower stratosphere but with somewhat lower values round the tropopause itself. Near the surface the SDs are much larger in northern mid-latitudes than southern mid-latitudes (also true in July) presumably reflecting the larger temperature variations over land. Tropical magnitudes are much less.

Relative humidity SDs (Fig. 4d) are quite low in the boundary layer rising to maxima in the upper troposphere; the gradient of the transition and the maximum values are rather large compared to our previous estimates from radiosonde minus background statistics. Pressure SDs (Fig. 4e) reduce with height (as might be expected given the reduction of pressure values), gradually in the troposphere then more rapidly in the stratosphere, magnitudes are much less in the tropics. Figure 4f shows that the pressure is largely balanced poleward of 30° below 100 hPa with the southern extratropics being slightly more balanced than the northern extratropics. There are several possible reasons for the dominance of the ageostrophic pressure in the stratosphere: a) the stratosphere may be intrinsically less geostrophic than the troposphere, b) the longer horizontal scales in the stratosphere imply that we should be calculating balanced winds from the mass field rather than vice versa, c) numerical noise due to the proximity of the top of the model or the vertical interpolations performed. These issues will be investigated further.

The January SDs shown are reasonably symmetric about the equator — extratropical errors tend to be larger in winter than summer, but overall errors are smaller in the northern extratropics than the southern extratropics. In July (not shown) there is significant asymmetry with the largest SDs in the southern extratropics.

Brief comparison has been made with root mean square (RMS) surface observation minus background (O-B) statistics for January 1999 (not shown) — the errors of the Synops and ships used should be independent of latitude to a first approximation. The wind RMS O-B magnitudes are smaller in the tropics than mid-latitudes. Temperature RMS differences show minima in the tropics and at 50–60 N/S separated by weak maxima. There are large temperature RMSs at high latitudes. The pressure RMS statistics are relatively flat between 50° S and 50° N. These results suggest that the lower SDs in the tropics seen in Fig. 4 are overstated, particularly for mass fields, probably because error growth rates (affecting the T+24 and T+48 forecasts) are lower in the tropics.

The u component of the wind has very narrow vertical correlations in the tropics, Fig. 5a shows the correlation with level 11 (approximately 500 hPa). In the extratropics there are much broader vertical scales with positive correlations extending almost to the top of the model. Looking at correlation greater than 0.6 the vertical scale tends to increase at higher latitudes and is largest in the southern hemisphere. In July (not shown) the vertical scale is even larger in high southern latitudes, but is fairly similar elsewhere. u_{div} has much narrower vertical correlations (Fig. 5b) which are approximately independent of latitude, but show some narrowing near the equator and some broadening over Antarctica.

Temperature (Fig. 5c) shows a distinct narrowing in the tropics, in the extratropics the correlations with level 11 are positive throughout the troposphere, they change sharply at the tropopause, with correlations down to -0.4 (or very locally -0.6) in the

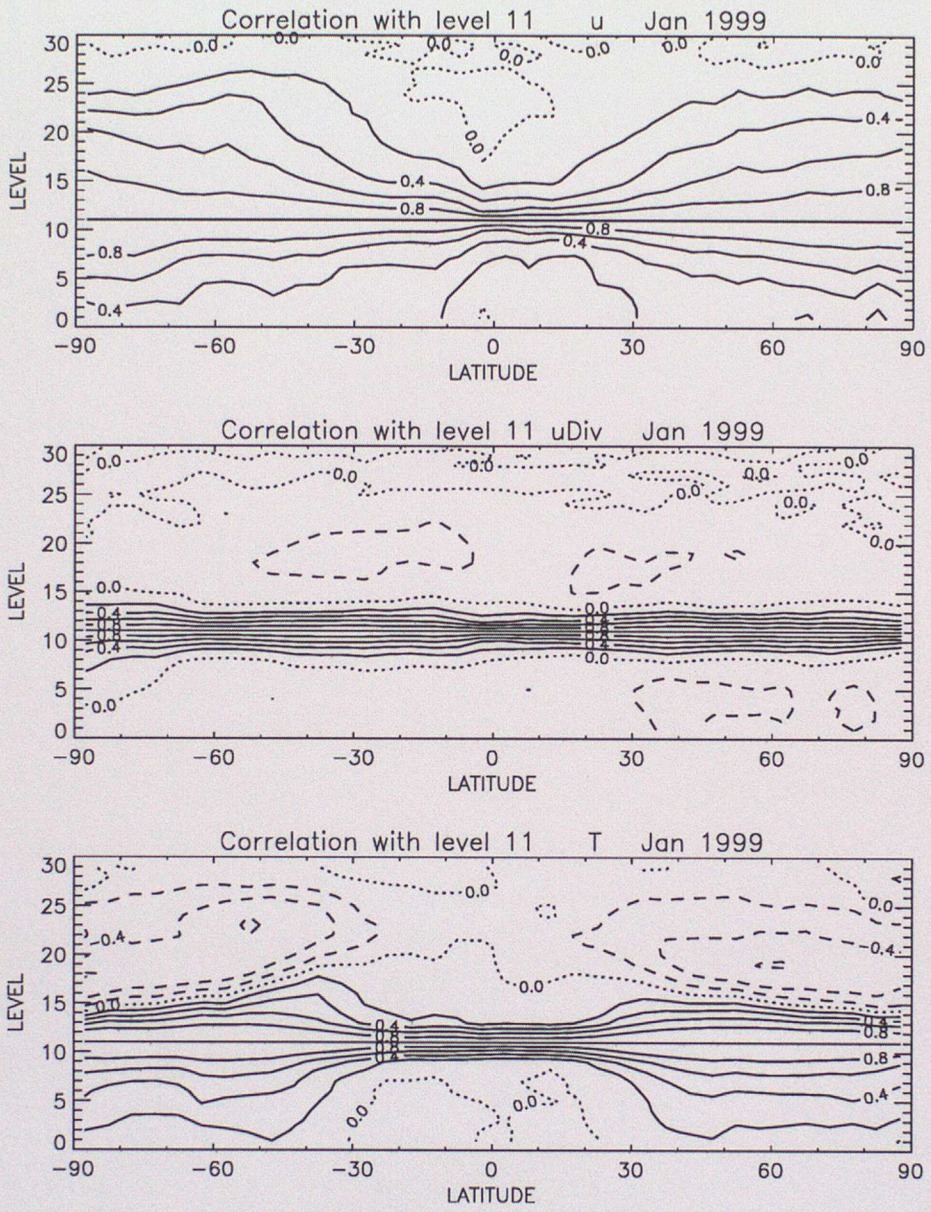

Figure 5. Vertical correlations of forecast differences with level 11 (approximately 500 hPa) for a) u, b) u_{div} and c) temperature.

lower stratosphere. In contrast with the generally positive vertical correlations of most variables such large negative correlations are quite notable, they were also found by Rabier *et al.* (1998, figure 12). The correlation between pressure differences at the top and bottom of the model is approximately zero, so that positive temperature correlations have to be compensated by negative correlations at a different level.

Pressure vertical correlations (not shown) are very broad but narrow slightly in the tropics. Relative humidity vertical correlations (not shown) are moderately narrow and

approximately independent of latitude, but with a slight narrowing about 20° N — also seen in previous versions of the statistics.

(*c*) *Mid-latitude vertical structure*

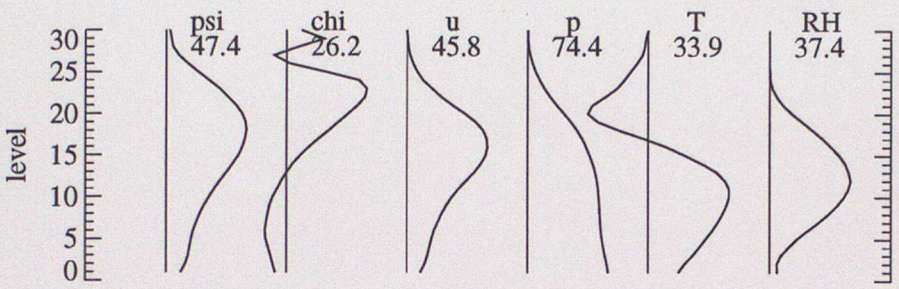

Figure 6. Dominant vertical global modes (see text for details) in arbitrary units. Calculated from forecast differences for July 1998 and January 1999.

Figure 6 shows the first vertical mode for various variables, and also the percentage of total variance explained. These are calculated as eigenvectors of the global vertical covariances, pressure weighted to take the mass of each layer into account; they are used in our representation of the background error covariances, see section 3 of Lorenc *et al.* (2000). (The percentage of total variance, and to a lesser extent the shape of the leading modes, are sensitive to the weighting used.) The global covariance matrices are dominated by the larger SDs in the extratropics, so the global modes are typical of mid-latitude conditions. The leading modes in particular appear to be physically meaningful, but they have somewhat larger scale than apparent in the correlations, see discussion in Richman (1986) and Jolliffe (1987).

The vertical modes have been calculated for the different variables independently, but for the largely balanced variables the leading modes are clearly interrelated to some extent. Looking at u we have an " 'equivalent barotropic' vertical structure with flow in the same sense at all levels and maximum amplitude near the tropopause" (Hoskins, 1987, p59). This will be in balance with (horizontally displaced) temperature perturbations of different sign in the troposphere and stratosphere. The first streamfunction mode is similar to that for u, but the maximum is displaced upwards slightly and there is more amplitude in the stratosphere — these effects are due to the longer scales and hence larger streamfunction:KE ratio in the stratosphere (see table 1 and discussion). There is also some broadening in the vertical as streamfunction emphasises larger horizontal scales and hence larger vertical scales (see Fig. 2a). For pressure the first mode explains almost 75% of the total variance (Fig. 6), in the troposphere the magnitude increases gradually towards the surface (it is only partially in balance with the first wind mode).

Velocity potential has a negative lobe (expected as the vertically integrated divergence should be close to zero) and slightly odd structure in the stratosphere. Relative humidity has a mode of the same sign at all levels with a maximum in mid-troposphere. Together with temperature these have shorter vertical scales than u or pressure and also a smaller proportion of variance explained by the first mode.

(*d*) *Tropical aspects*

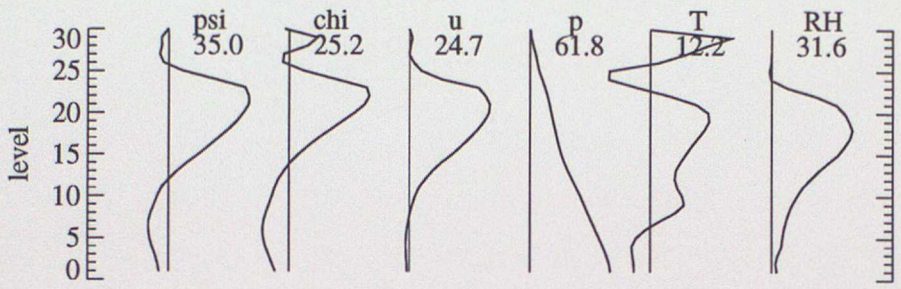

Figure 7. Dominant vertical tropical modes (see text for details). Forecast differences, July 1998 and January 1999.

Figure 7 shows leading vertical modes calculated just for the region between 15° south and 15° north, they are significantly different from the global modes in Fig. 6. The leading modes for streamfunction, velocity potential and u are quite similar and suggest strong flow in the upper troposphere associated with weak flow in the opposite direction at low levels (more so in v than u), similarly to Hoskins (1987). The leading pressure mode still dominates the pressure variance but has a simpler structure corresponding to a height pertubation appoximately constant in the vertical. The first temperature mode has a curious shape and only 12% of the variance, and is probably not physically meaningful. The first relative humidity mode has a broad maximum at about 250 hPa.

The vertical scales in the tropics are generally very short, but the small proportion of the tropics with deep convection, or particularly with tropical storms, will have much more coupling in the vertical. In the lower troposphere there are some indications of larger wind vertical scales at about 15° in the summer hemisphere (see Fig. 5a, although it is more noticeable at lower levels), which is tentatively identified with the effect of tropical cyclones.

In our system the regression applied to the 'balanced' pressure effectively removes the mass-wind coupling in the tropics as already shown in Fig. 4f. Daley (1996) notes that the equatorial u-height correlations for Rossby and Kelvin modes have opposite sign and may approximately cancel out. In our forecast differences collocated u-pressure correlations are generally less than 0.1 in magnitude within 10° of the equator although there are some positive correlations below 850 hPa and above 100 hPa (up to about 0.15 and 0.25 respectively).

(e) *Surface pressure/temperature correlations and polar regions*

Figure 8 shows correlations between p_* (model surface pressure) and temperature as a function of latitude. In mid-latitudes there are negative correlations in the lower-troposphere and upper-troposphere/lower-stratosphere with zero or slightly positive values in mid-troposphere. The negative correlation is strongest, -0.3 or locally -0.4, at about 900 hPa. In the tropics the correlations are generally slightly weaker. The most remarkable feature of Fig. 8 is the strong *positive* correlation of tropospheric temperatures with p_* over Antarctica, with some compensating negative correlations in the stratosphere above. There is some sign of a similar feature in the Arctic, but tropospheric correlations are close to zero. The positive correlation over Antartica is slightly weaker in July (not shown) when the low-level inversion and associated katabatic winds are stronger. The

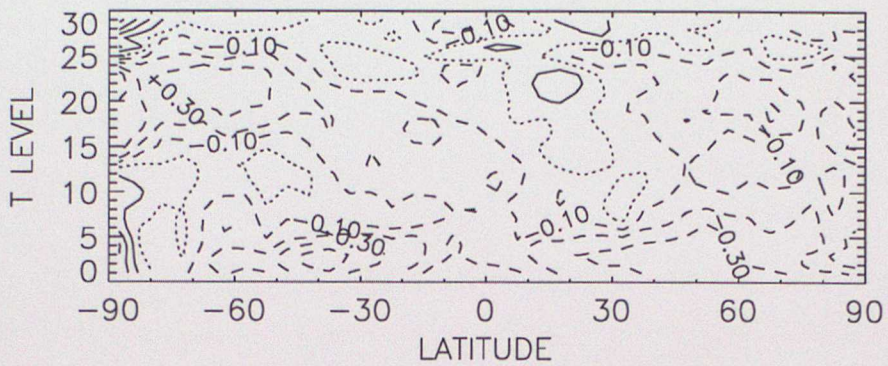

Figure 8. Correlation of surface pressure with temperature. Forecast differences, January 1999. Contour interval 0.1, with positive contours solid, zero contour dotted and negative contours dashed.

forecast difference statistics for the previous 19-level model did not have such positive correlations over Antarctica, but a comparison with observation-background covariances and the observational studies reported below suggest that the positive correlation is 'real'. Because of the various approximations made our 3D-Var does not represent the correlations in Fig. 8 exactly, but over Antarctica the low-level temperature correlations with p_* tend to be near zero rather than negative as they are at most latitudes.

In the AC scheme 'hydrostatic' potential temperature increments, of opposite sign and largest near the surface, were derived from the p_* increments (Lorenc et al, 1991). The negative rather than positive correlation at low levels was apparently responsible for some rather poor analyses at the South Pole in March/April 1998 shortly after the introduction of the 30-level model.

The synoptic relationship between pressure and temperature in the Antarctic winter is investigated by Wendler and Kodama (1993). They find significant positive correlation between surface temperature and pressure — 'at first glance a very astonishing result'. This appears to be at least partly due to occasional large-scale incursions of higher-latitude air. A very large warming of this type, associated with high pressure over East Antarctica, is documented by Enomoto *et al.* (1998). Perhaps the most obvious explanation among those suggested by Wendler and Kodama (1993) is that anticyclonic circulation is associated with descent and that for Antarctica (and to some extent the Arctic) the air aloft is relatively warm. The positive correlation of tropospheric temperature (errors) and surface pressure (errors) might be expected in any 'warm' anticyclone, including many extratropical blocking episodes.

On a seasonal time scale Antarctic surface temperature and pressure are positively correlated in that pressures are highest in summer. Parish and Bromwich (1997) note that seasonal temperature changes are largest in the stratosphere and near the surface and less in the middle and upper troposphere. They also note similarities with Greenland, and Rogers *et al.* (1997) describe an abrupt springtime temperature rise over Greenland in several years, preceeded by a significant pressure rise. The large scale nature of the phenomenon is consistent with Derber and Bouttier (1999), their figure 8 shows negative correlations in the lower troposphere at all scales except the very large ones, at large scales there are negative correlations at/above the tropopause and some positive correlations below.

3. Representing background error covariances and forecast experiments

(a) *Basic method*

The design of the J^b term is described briefly in section 3 of Lorenc *et al.* (2000) and it is partly based on that of Parrish and Derber (1992). We use the forecast difference statistics (section 2) for the 'control variables' (ψ, χ, Ap and RH). We calculate vertical modes from global vertical covariance matrices, and allow their variances to vary with latitude and season. For each vertical mode we calculate the horizontal correlation spectrum, but we replace these with SOAR (Second Order AutoRegressive) functions with related length scales. We then have to rescale the streamfunction and velocity potential variances so that the implied global kinetic energy is equal to that from the forecast differences.

(b) *Implied covariances*

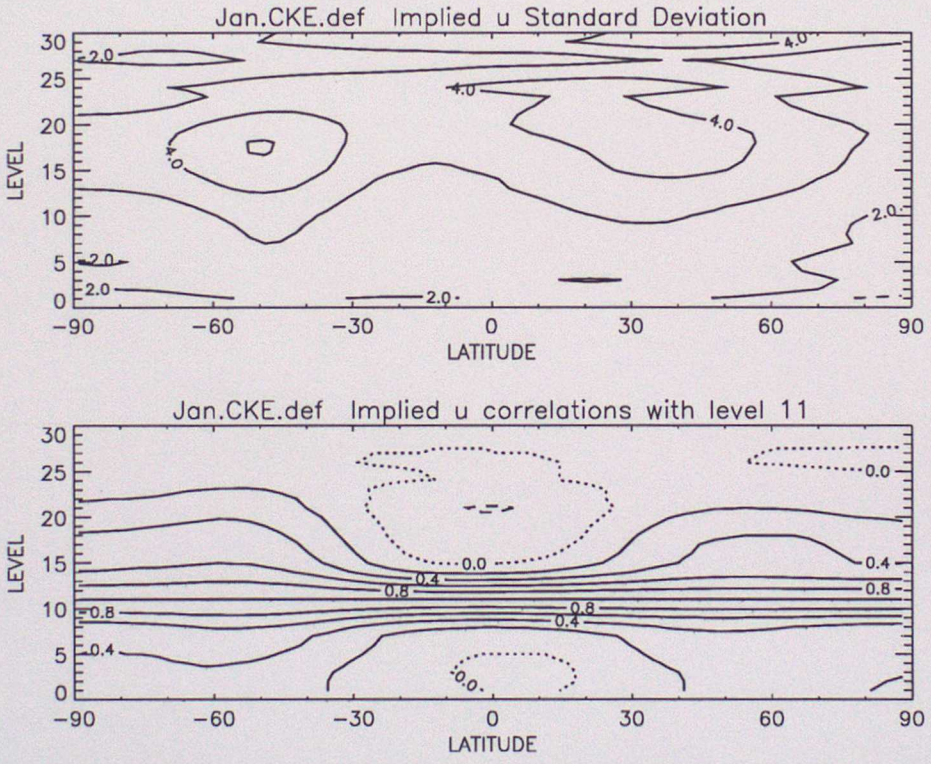

Figure 9. Implied u covariances for January. a) standard deviations as for Fig. 4a c) vertical correlations as for Fig. 5a

Figure 9a shows implied standard deviations (SDs) for u using the default options and can be compared with figure 4a. The main features are reasonably well captured: the mid-latitude jet level maxima are there but are slightly weak, SDs are weaker in the tropics as "observed" but somewhat too large below about 500 hPa (level 11). A feature that shows up slightly here is that the slope of the maxima with latitude is less

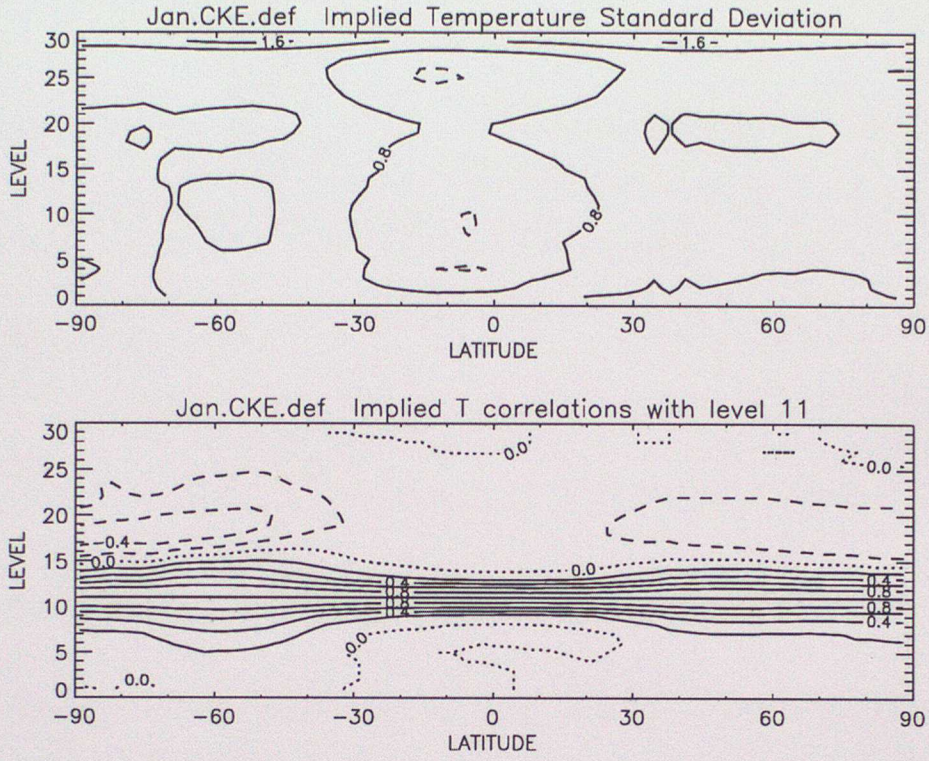

Figure 10. Implied T covariances for January. a) standard deviations as for Fig. 4c c) vertical correlations with level 11 as for Fig. 5c

marked than the "observed" slope which follows the tropopause; the dominant global mode is most representative of mid-latitudes and largely determines the location of the maximum. The implied vertical correlations with level 11 in figure 9b can be compared with figure 5a, as for the SDs the main features are present but somewhat smoothed and the implied vertical correlations in the tropics are narrow but not as narrow as in the forecast difference statistics. Implied temperature SDs, Fig. 10a, are less than those in Fig. 4c, partly due to the use of shorter ψ length scales. The vertical temperature correlations in Fig. 10b have shorter vertical scales and correspondingly less negative correlations in the stratosphere than Fig. 5c, but the gross features are similar.

The dominant equivalent barotropic mode is well modelled — it is probably most important in data sparse areas and may be exaggerated in the forecast differences relative to 6 hour forecast errors. Even if it is dominant over large areas of the globe there is an argument that it may be more important to get the analysis correct in the active baroclinic areas — this is part of the motivation for experimenting with shorter vertical correlations below.

Our system does represent the gross features of the relationship between vertical and horizontal scale for rotational wind (Fig. 11 compared to Fig. 2a), but horizontal length scales increase very little in the stratosphere and actually decrease somewhat for unbalanced pressure — Table 2. In the troposphere the lengths are somewhat less than those in table 1, this is due to the use of SOAR functions rather than direct use of the

TABLE 2. IMPLIED DIFFERENTIAL LENGTH SCALES (KM), SELECTED MODEL LEVELS, CF TABLE 1.

level	P	ψ	RKE	χ	DKE	Ap	RH
28	30	356	171	501	200	287	
25	102	306	160	344	169	323	179
19	251	356	171	380	174	357	192
11	519	352	169	320	161	401	199
4	867	339	168	353	167	404	190
2	961	325	164	331	163	373	185

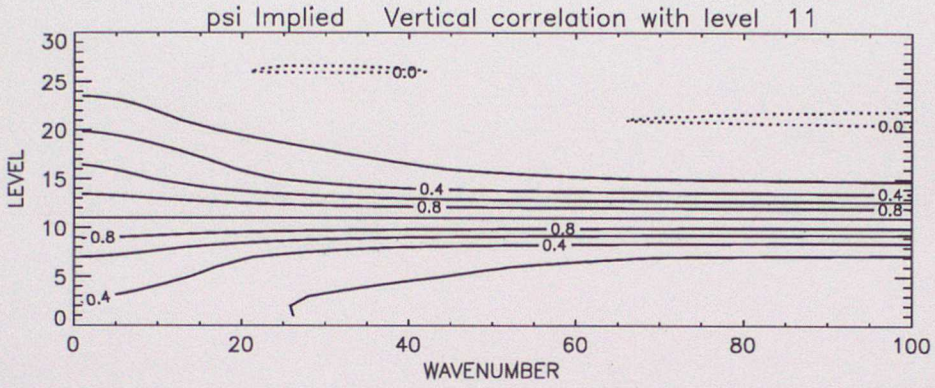

Figure 11. As Fig. 2 but implied vertical correlations for rotational wind.

forecast difference spectra.

The ability to (partly) represent the shorter vertical scales in the tropics is the main advantage of this system over the alternative of treating vertical correlations as a function of n. The revised ECMWF covariances (Derber and Bouttier, 1999) give somewhat shorter vertical temperature scales in the tropics than the extratropics, but the wind vertical correlations do not vary with latitude. As mentioned there is some evidence of longer scales in the tropics, and also in the Southern Hemisphere because of the data sparsity there. These are not catered for in the spectral representation of the horizontal correlations. In effect both systems are making modified separability assumptions, and neither of these can replicate the full three-dimensional structure seen in section 2.

(*c*) *Recent developments*

We briefly present four experiments that show the development of our covariance modelling over the last 18 months. Selected verification results are shown in Table 3. Experiments 1 to 3 use the previous sample of forecast differences based on 20 days each in July 1997 and January/February 1998. Experiment 1 (operational from late March to July 1999) used streamfunction and velocity potential vertical modes — all the others use rotational/divergent kinetic energy vertical modes which give slightly smaller vertical scales and a slightly better position of the wind variance maxima. Experiment 2 (our starting point in early 1998) differs in the scaling of streamfunction magnitudes and also has slightly larger vertical scales than experiment 3 (operational between late July and October 1999). In general experiment 3 appears better than 1 (tested on June 1999 data the impact was neutral) and 2 (although the impact is slightly negative measured

TABLE 3. RMS VERIFICATION AGAINST OBSERVATIONS AND ANALYSES FOR THE PERIOD 5 TO 19 MARCH 1999

Reference:	Observations				Analyses			
Experiment:	1	2	3	4	1	2	3	4
NH PMSL T+24	2.03	2.02	2.03	2.04	2.06	2.06	2.06	2.04
NH PMSL T+48	3.07	3.05	3.09	3.09	3.23	3.26	3.23	3.19
NH PMSL T+72	4.72	4.61	4.69	4.61	4.48	4.50	4.49	4.43
NH PMSL T+96	5.88	5.70	5.75	5.64	5.79	5.70	5.79	5.64
NH PMSL T+120	6.95	6.80	6.77	6.51	6.80	6.72	6.82	6.58
NH H500 T+24	1.88	1.88	1.88	1.85	1.58	1.59	1.55	1.53
NH H500 T+48	2.81	2.79	2.80	2.78	2.69	2.71	2.64	2.61
NH H500 T+72	4.26	4.27	4.22	4.17	4.03	4.05	4.00	3.91
NH W250 T+24	7.76	7.75	7.77	7.72	5.26	5.37	5.22	5.19
TR W850 T+24	4.01	4.01	4.00	4.00	2.20	2.19	2.15	2.18
TR W850 T+48	4.41	4.43	4.41	4.40	2.80	2.81	2.77	2.79
TR W850 T+72	4.61	4.63	4.64	4.59	3.23	3.25	3.22	3.23
TR W250 T+24	5.80	5.80	5.80	5.76	3.73	3.95	3.78	3.84
SH PMSL T+24	1.82	1.79	1.79	1.80	1.92	1.87	1.84	1.86
SH PMSL T+48	2.71	2.61	2.65	2.63	3.24	3.16	3.10	3.12
SH PMSL T+72	3.33	3.21	3.21	3.19	4.36	4.22	4.21	4.22
SH PMSL T+96	3.61	3.44	3.50	3.44	5.27	5.07	5.08	5.06
SH PMSL T+120	4.65	4.47	4.61	4.46	6.31	6.02	6.09	5.94
SH H500 T+24	2.09	2.15	2.11	2.02	1.77	1.76	1.66	1.68
SH H500 T+48	2.74	2.72	2.71	2.62	3.14	3.05	2.97	3.00
SH H500 T+72	3.65	3.65	3.57	3.48	4.33	4.17	4.19	4.13
SH W250 T+24	7.48	7.39	7.45	7.35	5.32	5.43	5.07	5.09
NH Skill	-0.12	0.09	46.77	0.25	-0.03	-0.02	47.93	0.32
TR Skill	-0.06	-0.11	4.11	0.12	0.00	-0.18	9.82	-0.07
SH Skill	-0.20	0.08	22.05	0.18	-0.32	-0.09	23.54	0.01

RMS verification against observations (TEMP and SYNOP reports) and analyses in hPa, dm and ms^{-1}. Skill scores (see Lorenc *et al.* (2000)) are given for experiment 3, and for the differences from experiment 3. Maximum possible skill scores are 56 for NH (20° to 90° north), 16 for TR (20° south to 20° north) and 28 for SH (20° to 90° south).

against observations).

Experiment 4 is essentially the same as experiment 3 but with more recent forecast difference samples (presented in section 2, they are slightly smoother and there are fairly subtle changes to the SDs and vertical correlations). This gives a modest improvement relative to 3, smaller when the experiment is extended for another week, with generally similar behaviour tested on June data. These statistics became operational in October 1999. The magnitude of the impact is comparable to major changes in observation usage.

(*d*) *Current and future work*

In the horizontal we have tried replacing the SOAR functions with correlations closer to those from the forecast differences, but made compactly supported (see Gaspari and Cohn (1998)). This effectively increases both horizontal and vertical length scales and has a definite positive impact on verification against observations, and a definite negative impact against analyses; the discrepancies are largest at short range and in the tropics. The change is generally beneficial in the southern hemisphere and at longer range.

We have performed some experiments using 'rotated' vertical modes (see eg Richman, 1986) in order to try to obtain more localised (and perhaps more physically meaningful) vertical modes. This does give longer horizontal scales, and better forecasts, in the stratosphere but the impact elsewhere is more mixed. These two changes have not been implemented operationally because of the mixed positive and negative results, but variants of them are likely to be tried again.

Acknowledgements

This work has depended on many people in the Met. Office VAR team in various ways including A. Lorenc, P. Andrews, S. Ballard, S. Bell, D. Barker, J. Bray, A. Clayton, M. Thurlow and others. In understanding the covariances conversations with, or information from, F. Bouttier, P. Courtier, M. Cullen, G. Desroziers, L. Fillion, M. Fisher, D. Parrish, F. Rabier and A. White have been useful, the latter provided helpful comments on the manuscript. My thanks are due to these and others for supplying pieces of the jigsaw.

References

Balgovind, R., Dalcher, A., Ghil, M., and Kalnay, E. 1983 A stochastic-dynamic model for the spectral structure of forecast errors. *Mon. Wea. Rev.*, **111**, 701–722

Bartello, P. and Mitchell, H. M. 1992 A continuous three-dimensional model of short-range forecast error covariances. *Tellus*, **44A**, 217–235

Boer, G. J. 1983 Homogeneous and isotropic turbulence on the sphere. *J. Atmos. Sci.*, **40**, 154–163

Boer, G. J. 1994 Predictability regimes in atmospheric flow. *Mon. Wea. Rev.*, **122**, 2285–2295

Bouttier, F. 1994 A dynamical estimation of forecast error covariances in an assimilation system. *Mon. Wea. Rev.*, **122**, 2376–2390

Charney, J. G. 1969 A further note on large-scale motions in the tropics. *J. Atmos. Sci.*, **25**, 182–185

Charney, J. G. and Drazin, P. G. 1961 Propagation of planetary-scale disturbances from the lower into the upper atmosphere. *J. Geophys. Res.*, **66**, 83–109

Daley, R. 1991 Atmospheric data analysis. Cambridge University Press

Daley, R. 1996 Generation of global multivariate error covariances by singular-value decomposition of the linear balance equation. *Mon. Wea. Rev.*, **124**, 2574–2587

Dee, D. and Gaspari, G. 1996 Development of anisotropic correlation models for atmospheric data assimilation. *Preprints, 11th Conf. on Numerical Weather Prediction*, Amer. Meteor. Soc., 249–251

Derber, J. and Bouttier F. 1999 A reformulation of the background error covariances in the ECMWF global data assimilation scheme. *Tellus*, **51A**, 195–221

Enomoto, H. Motoyama, H. Shiraiwa, T. Saito, T. Kameda, T. Furukawa, T. Takahashi, S. Kodama, Y. and Watanabe, O. 1998 Winter warming over Dome Fuji, East Antarctica and semi-annual oscillation in the atmospheric circulation. *J. Geophys. Res.*, **103**, 23103–23111

Gaspari, G. and Cohn, S. 1998 Construction of correlation functions in two and three dimensions. *Quart. J. R. Met. Soc.*, **125**, 723–758

Ghil, M. Halem, M. and Atlas, R. 1979 Time-continuous assimilation of remote sensing data and its effect on weather forecasting. *Mon. Wea. Rev.*, **107**, 140–171

Hollingsworth, A. and Lönnberg, P. 1986 The statistical structure of short-range forecast errors as determined from radiosonde data. Part I: The wind field. *Tellus*, **38A**, 111–136

Hoskins, B. J. 1987 Diagnosis of forced and free variability in the atmosphere. *Atmospheric and Oceanic Variability*, ed. H. Cattle, Royal Meteorological Society, 57–73

Ingleby, N. B. and Bromley, R. A. 1990 Model error structure and estimated analysis accuracy with a network of wind profilers. *Meteorologische Rundschau*, **42**, 83–93

Jiang, S and Ghil, M. 1993 Dynamical properties of error statistics in a shallow water model. *J. Phys. Oceanogr.*, **23**, 2541–2566

Jolliffe, I. T. 1987 Rotation of principal components: some comments. *J. Climatol.*, **7**, 507–510

Lindzen, R. S. and Fox-Rabinovitz, M. 1989 Consistent vertical and horizontal resolution. *Mon. Wea. Rev.*, **117**, 2575–2583

Lönnberg, P. and Hollingsworth, A.	1986	The statistical structure of short-range forecast errors as determined from radiosonde data. Part II: The covariance of height and wind errors. *Tellus*, **38A**, 137–161
Lorenc, A. C., Ballard, S.P., Bell, R. S., Ingleby, N. B., Andrews, P. L. F., Barker, D. M., Bray, J. R., Clayton, A. M., Dalby, T., Li, D. and Payne, T. J.	2000	The Met. Office Global 3-Dimensional Variational Data Assimilation Scheme. *submitted to Quart. J. Roy. Met. Soc.*
Milton, S. F., and Wilson, C. A.	1996	The impact of parameterized subgrid-scale orographic forcing on systematic errors in a global NWP model. *Mon. Wea. Rev.*, **124**, 2023–2045
Lorenc, A. C., Bell, R. S., and Macpherson, B.	1991	The Meteorological Office "Analysis Correction" data assimilation scheme. *Quart. J. Roy. Met. Soc.*, **117**, 59–89
Mitchell, H. M., Charette, C., Chouinard, C., and Brasnett, B.	1990	Revised interpolation statistics for the Canadian data assimilation procedure: their derivation and application. *Mon. Wea. Rev.*, **118**, 1591–1614
Parish, T. R. and Bromwich, D. H.	1997	On the forcing of seasonal changes in surface pressure over Antarctica. *J. Geophys. Res.*, **102**, 13785–13792
Parrish, D. F. and Derber, J. C.	1992	The National Meteorological Center's Spectral Statistical Interpolation analysis system. *Mon. Wea. Rev.*, **120**, 1747–1763
Rabier, F., McNally, A., Andersson, E., Courtier, P., Undén, P., Eyre, J., Hollingsworth, A. and Bouttier, F.	1998	The ECMWF implementation of three-dimensional variational assimilation (3D-Var). II: Structure functions. *Quart. J. R. Met. Soc.*, **124**, 1809–1829
Richman, M. B.	1986	Rotation of principal components. *J. Climatol.*, **6**, 293–335
Rogers, J. C. Hellstrom, R. A. Mosley-Thompson, E. and Wang, C-C.	1997	An abrupt spring air temperature rise over the Greenland ice cap. *J. Geophys. Res.*, **102**, 13793–13800
Tomas, R. A. and Webster, P. J.	1994	Horizontal and vertical structure of cross-equatorial wave propagation. *J. Atmos. Sci.*, **51**, 1417–1430
Wendler, G. and Kodama, Y.	1993	The kernlose winter in Adelie coast. in 'Antarctic Meteorology and Climatology' ed D.H.Bromwich and C.R.Stearns, *Antarctic Res. Ser.*, **61**, 139–147